Parametric Study on Seismic Behaviour of Exterior Reinforced Concrete Flat Plate Column Connection

Abhijeet Kashliwal
AFCONS Infrastructure Limited, Mumbai, India

Kaustubh Dasgupta
Department of Civil Engineering, Indian Institute of Technology Guwahati, India

SUMMARY

Although the popularity of Reinforced Concrete (RC) flat plate systems is on the rise, but their weakness in punching shear capacity makes their application questionable, especially under large seismic drifts. To understand the basic failure modes and shear stress transfer in column-flat slab connections, nonlinear finite element method of analysis is adopted in the present study. Using layered finite element modeling technique, the influence of various parameters, namely (a) aspect ratio of connection, (b) depth to span ratio and (c) spacing of stirrups (change in lateral confining pressure on concrete), governing the punching shear capacity of the connection, is also discussed to understand the seismic behavior under large lateral displacements. With this study, realistic values of punching shear capacity of the connections and acceptable drift limits for the safe functioning of the RC flat plate buildings particularly in severe seismic zones have also been suggested. Finally, the procedure for developing performance curves is also discussed by varying the gravity-shear ratio.

Keywords: Flat plate, punching shear, seismic drifts, layered finite element, and gravity-shear ratio.

1. INTRODUCTION

The simplest definition of Flat Plate Systems can be stated as "Buildings in which slabs are supported directly on columns". Flat plate systems have become increasingly popular in today's world of construction due to its certain distinct advantages – economy, speedy construction and aesthetic beauty. As such, RC flat-plate systems have become quite a common sight in most of the developing countries, including India. But, the weakness of such systems in punching shear makes their application questionable, especially in seismic prone areas. It is found that under large seismic displacements of the structure, punching shear stresses increases dramatically in the vicinity of plate-column connection leading to abrupt and progressive failure of the system (Kuang and Morley, 1992; Park and Choi, 2006; Yankelevsky and Leibowitz, 1995; Zhang, 2002). Under earthquake loading, the conventional structural analysis approaches, namely plasticity and octahedral shear stress models, have not been able to capture comprehensively the observed punching shear failure modes. For a better explanation of failure modes and shear stress transfer in column-flat slab connections, nonlinear finite element method of analysis is adopted in the present study. Using layered finite element modeling technique the influence of various parameters, governing the punching shear capacity of the connection, is highlighted.

2. PRESENT CASE STUDY

Hypothetical six storied "residential type" open ground RC flat plate building is considered in the present study. The size of column is 400mm×400mm and slab (or plate) of overall depth 200 mm is taken (common for both roof plate and floor plate). Thickness of brick masonry infill walls is taken as 230mm. The unit weight of concrete is taken as 25 kN/m^3.

3. MODELING OF FLAT PLATE BUILDING

The modeling of the hypothetical flat plate building is carried out in SAP2000 V14.0 (CSI, 2009).

The plates and the reinforcement bars are modeled as nonlinear isoparametric four noded shell elements using the concept of layered finite element technique while columns are modeled as linear frame elements (Figure 3.1).

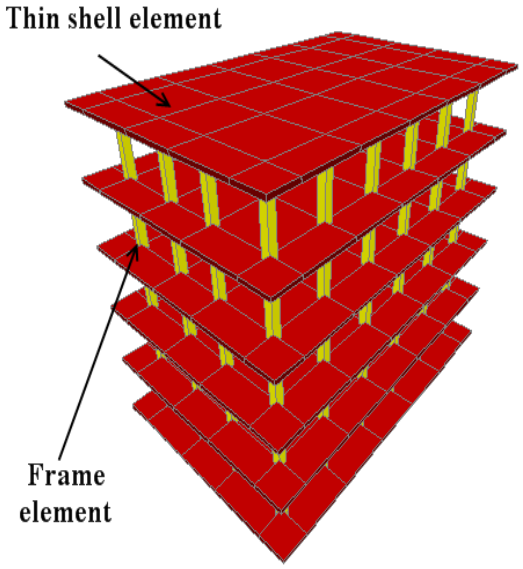

Figure 3.1. Perspective view of the entire RC Flat Plate Building

3.1 Layered Finite Element Technique

The plates and longitudinal reinforcement of the flat plate building are modeled as four noded isoparametric shell element. These reinforcement shell layers are superimposed on the concrete layers. The material properties of steel are assigned to these shell elements. It is also possible to model reinforcement using rebar or membrane element. But, these models do not produce realistic deformed shape during modal analysis. So, to ensure compatibility with the overall behaviour of structure, it is proper and logical to model the reinforcement as shell element. In the layered shell element, the reinforcement is modeled as a smeared (continuous) layer (Figure 3.2a). But, in reality the longitudinal reinforcement are put at a finite spacing. To produce the effect of spacing, the diameter of longitudinal reinforcing bars were reduced and a shell with reduced thickness is employed in such a way that the total cross sectional area of longitudinal reinforcement is conserved.

3.2 Modeling of material behaviour

3.2.1 Unconfined concrete

In the present study, the Saatcioglu and Razvi model (Saatcioglu and Razvi, 1992) for unconfined concrete is used (Figure 3.2b). The unconfined concrete compressive strength (f_{uc}) is expressed as

$$f_{uc} = f_{cc}\,[2\frac{\varepsilon_c}{\varepsilon_{01}} - (\frac{\varepsilon_c}{\varepsilon_{01}})^2] \quad \text{for} \quad 0 \le \varepsilon_c \le \varepsilon_{01} \tag{3.1}$$

$$f_{uc} = f_{cc}\,[1 - \frac{0.15(\varepsilon_c - \varepsilon_{01})}{\varepsilon_{085} - \varepsilon_{01}}] \quad \text{for} \quad \varepsilon_c \ge \varepsilon_{01} \tag{3.2}$$

where, f_{uc} = unconfined concrete compressive strength at any strain ε_c (MPa), f_{cc} = maximum compressive stress (MPa), ε_c = direct compressive strain; ε_{01} = strain at peak unconfined compressive strength (0.002) and ε_{085} = strain at 85% of f_{cc} (0.0038).

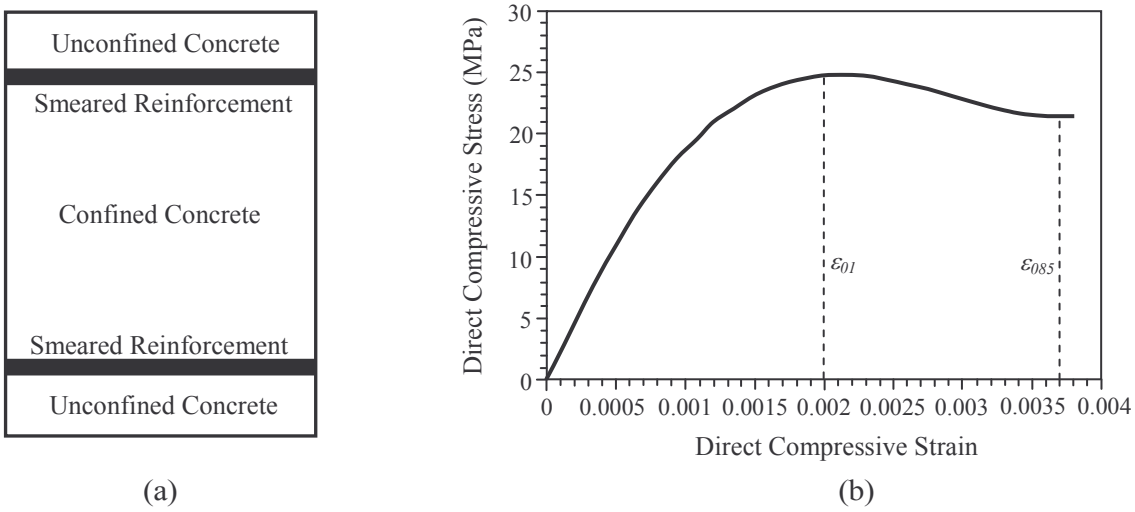

Figure 3.2. (a) Layered finite element model for flat plate reinforced concrete section, and (b) direct stress strain model for unconfined concrete

3.2.2 Confined Concrete

Many mathematical models have been proposed to quantify the effect of confinement and henceforth to define the stress strain curve for the confined concrete. The prominent models being the Mander model, Hoshikuma model and Saatcioglu and Razvi model. Hoshikuma model is totally based on regression analysis of experimental data. This makes its applicability quite difficult in practical situations where it may not be possible to simulate similar test conditions. The limitation of the Mander model lies in its complex expression of the orthogonal confining pressures that exists in rectangular sections. Unlike the square sections, in rectangular concrete sections, the confining pressures are different in the two orthogonal directions. Thus we need to have an equivalent effect of these two different confining pressures. Here, the Mander model induces some errors and it is not possible to implement the same in computer. The numerical expressions of Saatcioglu and Razvi model clearly reflect the exact mechanics of confining action under two different lateral pressures. The model follows a simple averaging technique to combine the confining pressures in the two orthogonal directions of the rectangular sections. The procedure recognizes potential differences in confinement pressures in two orthogonal directions, and allows for superposition of confinement effects of different types and arrangements of reinforcement. The model is based on equivalent uniform confinement pressure generated by the reinforcement cage.

The present case study takes into consideration Saatcioglu and Razvi model to model the effect of different confining pressures (*i.e.*, effect of different spacing of stirrups) in concrete sections. In this model, the confined concrete (f_{cc}) compressive strength is expressed as (Figure 3.3)

$$f_{cc} = f_{cc}'\left[2\frac{\varepsilon_c}{\varepsilon_1} - \left(\frac{\varepsilon_c}{\varepsilon_1}\right)^2\right]^{\frac{1}{1+2k}} \quad \text{for} \quad 0 < \varepsilon_c \leq \varepsilon_1 \tag{3.3}$$

$$f_{cc} = f_{cc}'\left[1 - \frac{0.15(\varepsilon_c - \varepsilon_1)}{\varepsilon_{85} - \varepsilon_1}\right] \quad \text{for} \quad \varepsilon_1 < \varepsilon_c \leq \varepsilon_{20} \tag{3.4}$$

$$f_{cc} = 0.2\, f_{cc}' \quad \text{for} \quad \varepsilon_c > \varepsilon_{20} \tag{3.5}$$

Here,

$$k = \frac{k_1 f_{le}}{f_{co}'} \quad , \qquad k_1 = 6.7\ (f_{le}\ )^{-0.17} \quad , f_{le} = \frac{\sum A_s\ f_{yt}}{b_c\ s}\ ,\ f_{leqv} = k_2\ f_{le} \text{ and } k_2 = .26\sqrt{\frac{b_c}{s}\frac{b_c}{s_1}\frac{1}{f_l}}$$

f_{le} = lateral confinement pressure (MPa), f_{co}' = unconfined compressive strength of concrete (MPa), A_s = cross sectional area of lateral ties, b_c = width of concrete section, S = spacing of lateral ties, $\varepsilon_1 = \varepsilon_{01}\ (1 + 5k)$, $\varepsilon_{01} = .002$ and $\varepsilon_{85} = 260\ \rho_s\ \varepsilon_1 + \varepsilon_{085}$, $\varepsilon_{085} = .0038$.

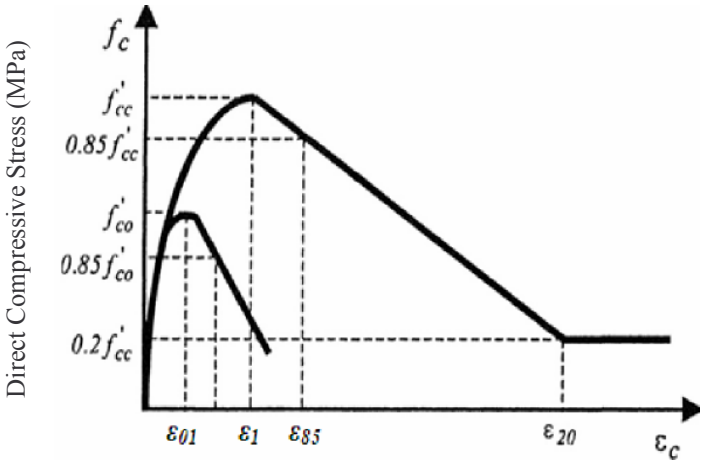

Figure 3.3. Confined concrete stress strain curve (Kashliwal, 2011)

Finite element modeling of stirrups or lateral ties has always been a difficult and cumbersome task. Very few finite element software packages provide this facility and even if they provide the degree of precision of modeling remains a question mark. Thus, instead of directly modeling the stirrups, it is better to model the effect that stirrups have on the concrete section using available numerical models. The stirrups or lateral ties increases the lateral confining pressure on the concrete section as a result of which the compressive strength gets enhanced. In view of this, the above model is employed.

3.2.3 Shear behaviour in concrete

The computation of shear capacity is based on Mohr's philosophy of maximum shear stress which states that "the maximum shear stress acts at an angle of 45 degrees from the major axis". But, in practical loading conditions, concrete has multiple modes of failure (flexure failure, shear failure, diagonal tension failure etc) and the actual failure pattern may consists of a dominant single mode or combination of all the modes. Hence, in general, it is very difficult to assess actual shear capacity of concrete. Thus, to ascertain the true shear capacity of a concrete section, a dummy model of concrete is devised (Figure 3.4).

In this model, the concrete is assumed to have equal flexural capacity in both tension and compression. In other words, concrete is strengthened in flexure so that the predominant failure occurs in shear mode. This model thus restricts the flexural failure in concrete and thereby ensures that the failure of concrete section is solely governed by shear (or diagonal tension failure). This dummy model of concrete in shear is based on Saatcioglu and Razvi stress-strain curve (Figure 3.5).

4. ANALYSIS METHODOLOGY

4.1 Pushover Analysis

Pushover analysis is a stepwise nonlinear static analysis primarily used to monitor the response

of a structure (punching shear variation/flexural hinge state) at every step. Pushover analysis is essentially involves two steps. In the first step, the response of the structure is monitored only

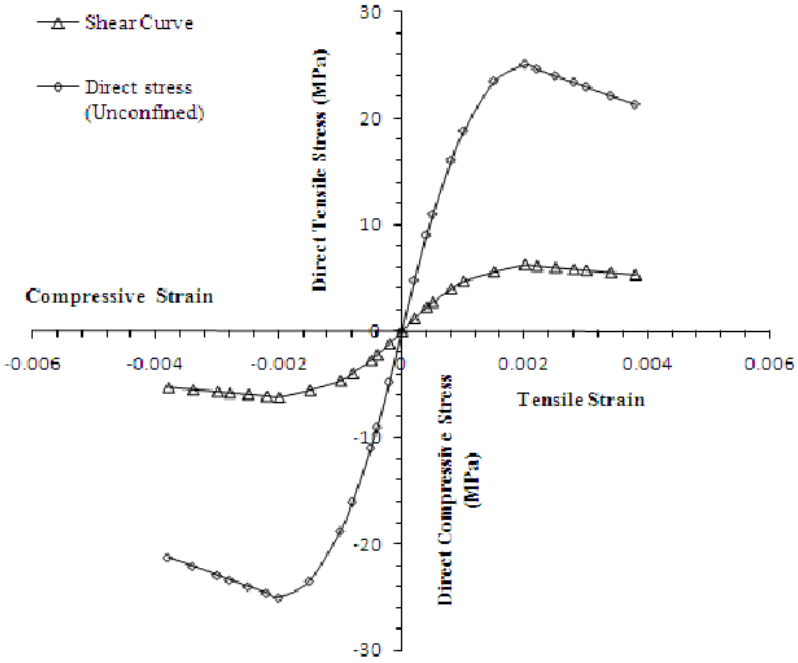

Figure 3.4. Stress-strain models for shear in concrete

under vertical loads (*DL + LL*). Then, the structure is slowly displaced in the direction of lateral (earthquake) load with the vertical load always acting in the laterally deformed structure. In pushover analysis, it is a usual practice to apply the push (or load) in the form of modal shape (fundamental mode). Pushover Analysis is primarily of two types: a) Displacement Control b) Force Control.

4.1.1 Displacement Control

Displacement control pushover analysis is undertaken to estimate the ductility of the structure. It is used to monitor the behaviour of hinges, moments, base reaction etc with increase in lateral drift. In the present study, displacement control pushover analysis is performed using SAP 2000 program. On performing nonlinear static pushover analysis, the behaviour of punching shear capacity of the plate-column connection is monitored at each step.

4.1.2 Force Control

Force control pushover analysis is undertaken to see up to what level of force (*i.e.*, lateral load) the system behaves elastically. Once, the structure reaches plastic state, and then the force control pushover analysis fails, as the load carrying capacity of the structure becomes constant. To monitor the behaviour beyond plastic state, displacement control pushover is again used. Thus, force control push over analysis is basically performed in case of linear analysis.

5. PARAMETRIC STUDY OF PUNCHING SHEAR STRENGTH

In the parametric study, the displacement values (Δ) of the building are normalized with respect to height of the building (H_b) and punching shear capacity of the flat-plate exterior column connection (τ) are normalized with respect to design shear strength of connection ($\tau_c = 0.25\sqrt{f_{ck}}$) as per Indian Concrete Code IS:456 (IS:456, 2005). The shear capacity curve so obtained is based on the shear stress model as discussed earlier which ensures that flexural yielding does not occur anywhere in the

vicinity of connection a priori. In other words, the only mode of failure available in concrete section is shear failure.

5.1 Aspect Ratio

For a particular gravity shear ratio (GSR), grade of concrete and thickness of plate, the punching shear capacity of connection is obtained with varying aspect ratio of column (Figure 5.1). The aspect ratio is varied only by changing the width of the column. The depth of the column (in the direction of pushover) is kept the same. With an increase in aspect ratio of column β (= longer dimension/ shorter dimension), the punching shear strength around the flat plate column connection decreases till the peak shear strength is reached. Beyond the peak shear strength, the trend reverses. Beyond peak strength, the shear capacity of the connection having the least aspect ratio falls steeply in comparison to the connection having larger aspect ratios. With increase in aspect ratio, it is found that the peak shear strength shifts towards right – the peak occurs at higher values of lateral drift.

In other words, connections with high aspect ratios (β = 1.5 and 2) appear to be more ductile in comparison to connections with low values of aspect ratio (β = 1). From the graph it is evident that the maximum shear capacity is achieved in a drift range of 2.5% to 3%. The peak shear strength is found to be of the order of 2.5 to 3 times of design shear capacity of connection (τ_c). The post peak shear strength of connection is higher for connections having larger aspect ratios. For low aspect ratio (β = 1), the post peak strength falls steeply while connection with higher aspect ratio of columns showed a gradual decline in strength. The plot revealed a very important observation regarding the elastic drift limit (drift up to which the punching shear strength varied almost linearly). The punching shear capacity is seen to vary linearly up to a lateral drift of about 1% before the curve goes into the non-linear zone. This shows that the code-prescribed elastic drift limit of 0.4% underestimates the actual behaviour.

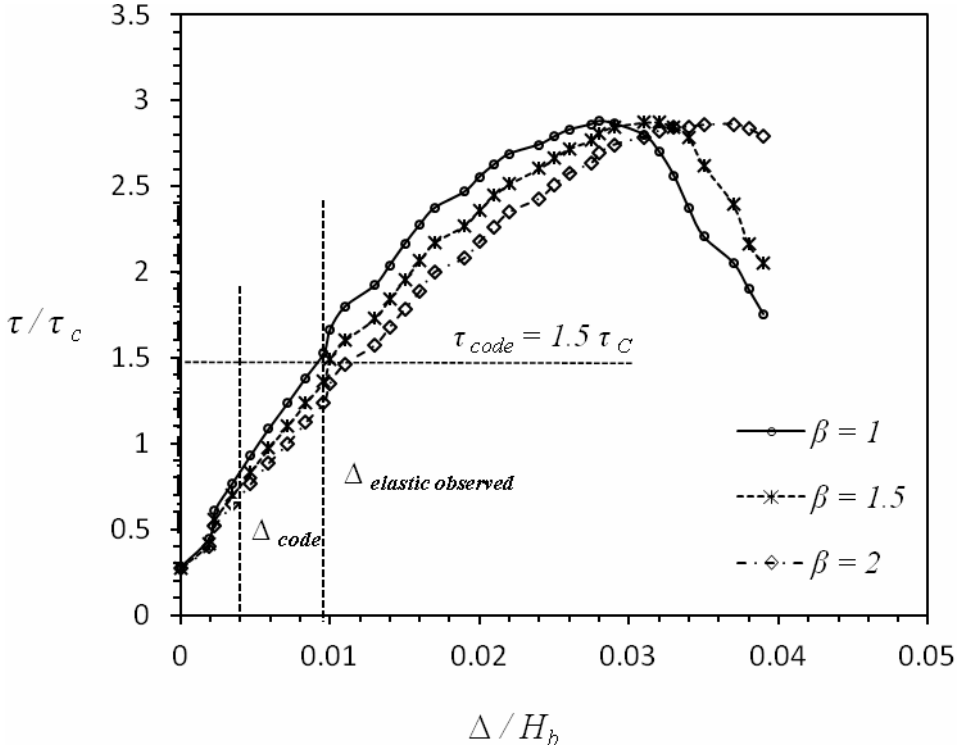

Figure 5.1. Punching shear capacity of flat-plate edge column connection with varying aspect ratio

5.2 Span to Depth Ratio

For a particular or predefined GSR, grade of concrete and aspect ratio of column, the punching shear

capacity of connection is obtained with varying span to depth ratio of flat plate (Figure 5.2). The shear capacity increased with increasing ratio of overall depth to span (*d/L*). The shear capacity of the connection is found to be highest for *d/L* = 0.15 with a value equal to 4.8 τ_c and the least was observed for *d/L* = 0.03 (1.5 τ_c). But, beyond the peak shear strength, the trend reverses; the shear capacity of the connection with higher depth to span ratio (*d/L* = 0.08 to 0.15) fails abruptly with zero post peak shear capacity. On the other hand, post peak strength of connections with lower values of depth to span ratio (*d/L* = 0.03 to 0.07), is found to degrade gradually and showed significant ultimate shear capacity. The ultimate shear capacity was found to be highest for *d/L* = 0.05, with a value equal to 1.8 τ_c. The depth to span ratio equal to 0.08 is found to be the critical *d/L* ratio. For values of *d/L* less than 0.08, the punching shear capacity of the connection showed a ductile trend while for d/L values above 0.08, the connection appeared to undergo abrupt failure in shear. Thus, we can define a dimensionless parameter "c_{dr}" as ratio of (*d/L*)/0.08. Mathematically, c_{dr} = 12.5 *d/L*. If c_{dr} < 1, mode of punching shear failure is ductile, if c_{dr} = 1, the failure mode can be either of the two and for c_{dr} > 1 the mode of failure is brittle. Further, it may be added that for very low values of depth to span ratio (*d/L* = 0.03), the difference between the peak shear capacity and the ultimate shear capacity of the connection is found to be minimal, *i.e.* the punching shear behaviour of the connection appears to be absolutely ductile. From the above discussion, it is evident that connection with high values of *d/L* fails abruptly while the one with low *d/L* ratio shows a ductile mode of failure. In thick plates (high *d/L* ratio), the load transfer takes place predominantly by strut action. This results in very high concentration of stresses at the junction leading to sudden shear failure. While for lower *d/L* ratios substantial portion of load from plate to connection gets transferred by flexural action as such ductile failure mode dominates.

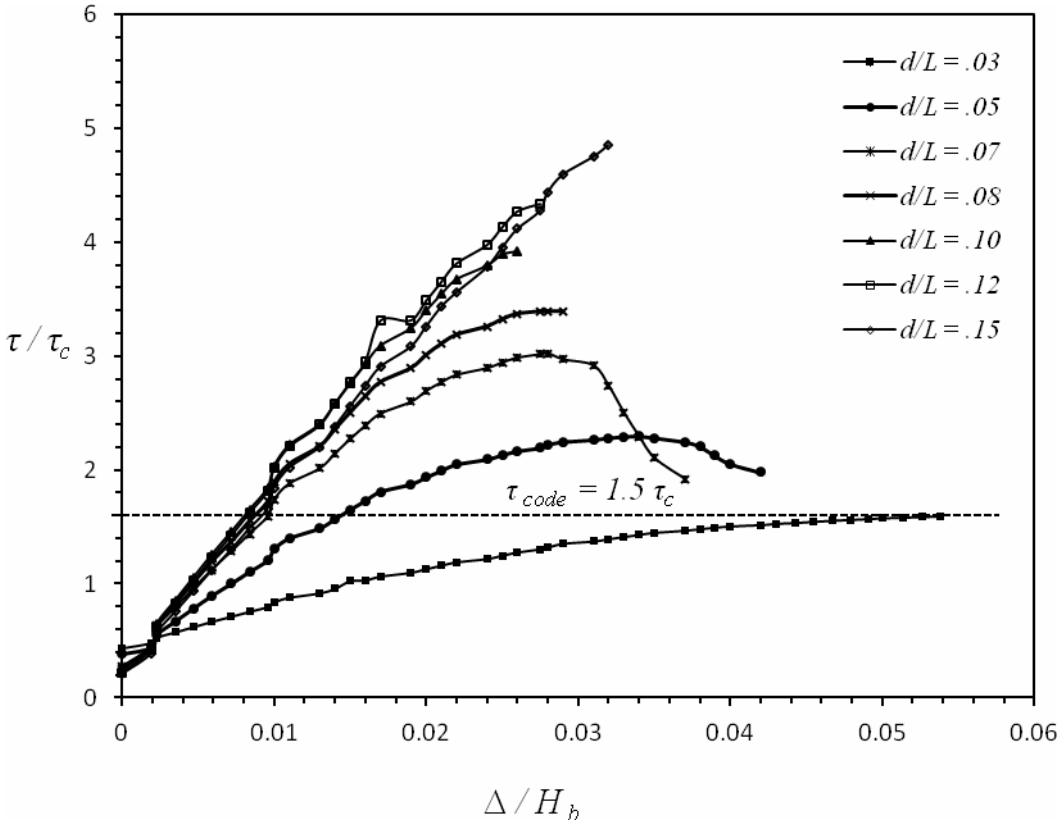

Figure 5.2. Punching shear capacity of edge plate column connection with varying depth to span ratio

The lateral drift capacity, Δ_{max} (drift at ultimate failure) showed a decreasing trend up to critical depth to span ratio (i.e *d/L* = 0.08, c_{dr} = 1) with *d/L* = 0.03, having the highest drift capacity equal to 5%. For c_{dr} > 1, the trend reverses as Δ_{max} increases with increase in the value of *d/L*. For *d/L* = 0.10, Δ_{max} is found to be 2.7% and for *d/L* = 0.15, Δ_{max} = 3.2%. The important observation here is regarding the elastic drift limit. Irrespective of the depth to span ratio, the elastic drift limit ($\Delta_{elastic}$) is observed to be

around 1% of height of the building; this is nearly twice the drift limit prescribed by the Indian earthquake code IS:1893 (Part 1) [IS:1893 (Part 1), 2002]. This value of $\Delta_{elastic}$ is same as that found in the previous section, indicating $\Delta_{elastic}$ is independent of the geometry of the connection. From the above discussion, it can be concluded that, the strength of the connection increases with increasing values of *d/L* but the ductility degrades.

5.3 Confinement Pressure

For a particular shear ratio, grade of concrete, depth to span ratio and aspect ratio of column, the punching shear capacity of connection is obtained with varying confinement pressure (Figure 5.3). The variation in confinement pressure was obtained by varying the spacing of stirrups in the connection region. The shear capacity of the connection increased with increase in lateral confinement pressure around the concrete (i.e. with decrease in spacing of stirrups). The peak shear capacity of the connection raised to as high as 4 times the design shear strength (τ_c) for 50 mm center to center spacing of stirrups. For spacing of stirrups equal to 100 mm, 150 mm and 200mm, this value was observed to be in the range of 3.25 times to 3.75 times τ_c. On the other hand for unconfined concrete the peak shear capacity was merely 2.5 times the design strength. Post peak strength also increased with decrease in the spacing of stirrups. The lateral drift capacity, Δ_{max} showed an interesting behaviour. It was found to be independent of the confinement pressure and was observed to be around 6%. However, the lateral drift till peak strength (Δ_{peak}) varied with spacing of stirrups. With increase in spacing of stirrups, Δ_{peak} decreased. For 50 mm spacing of stirrups, Δ_{peak} value was observed to be highest (6%) followed by 5%, 4.5 % and 4% for 100mm, 150 mm and 200 mm spacing of stirrups respectively. For unconfined concrete, this value was observed to be 2.5%. Like, the previous two cases, here too $\Delta_{elastic}$ is found to be in the range of 1% irrespective of the confinement pressure, indicating that $\Delta_{elastic}$ is not only independent of the geometry of the connection but also independent of confinement pressure. From the above discussion, we can conclude that with decrease in spacing of stirrups or increase in confinement pressure, both the strength and ductility of the connection enhanced.

5.4 Shear Demand of Flat Plate-Edge Column Connection

In the following results, the global lateral displacement values (Δ) of the building are normalized with respect to height of the building (H_b) and the shear stress demands (τ_d) of the flat plate exterior-column connection are normalized with respect to design shear strength of connection (τ_c). The shear demand curve so obtained is based on the shear stress model as shown in Figure 3.4. Figure 5.4 displays the variation of τ_d with gravity shear ratio (*GSR*) for a particular grade of concrete, depth to span ratio and aspect ratio of column. The shear demand of the connection increases with increase in gravity shear ratio, *GSR* (ratio of gravity shear to punching shear capacity at the connection). For *GSR* = 0.50, the shear demand is found to be maximum (2.8 τ_c). Greater the shear demand, greater the capacity of the connection required.

5.4.1 Performance Point

Overlapping shear demand curve, with the capacity curves as discussed in the previous sections, may give a good insight into the preliminary selection of geometry and shear design details of the connection. For a particular GSR and aspect ratio, the point where the shear demand curve meets the capacity curve may be termed as the performance point.

6. CONCLUSIONS

Aspect ratio, span to depth ratio and confining pressure showed significant influence on the punching shear capacity of the flat plate column connection. Connections with high aspect ratios appear to be more ductile in comparison to connections with low values of aspect ratio. The shear capacity

increased with increasing overall depth by span ratio. For values of *d/L* less than 0.08, the punching shear capacity of the connection showed a ductile trend while for *d/L* values above 0.08, the connection appeared to undergo abrupt failure in shear. The lateral drift capacity, Δ_{max} (drift at ultim-

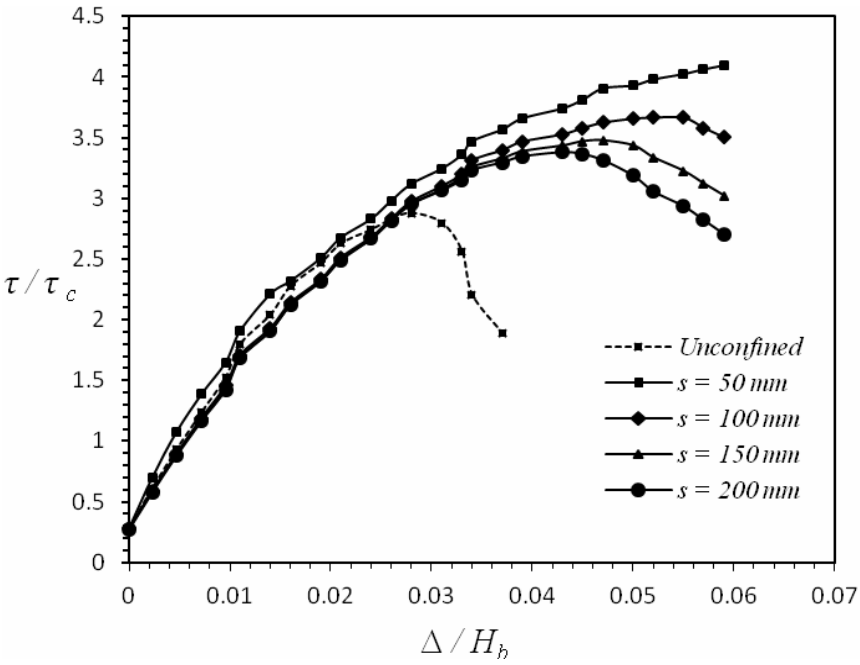

Figure 5.3. Punching shear capacity of edge flat plate column connection with confinement pressure

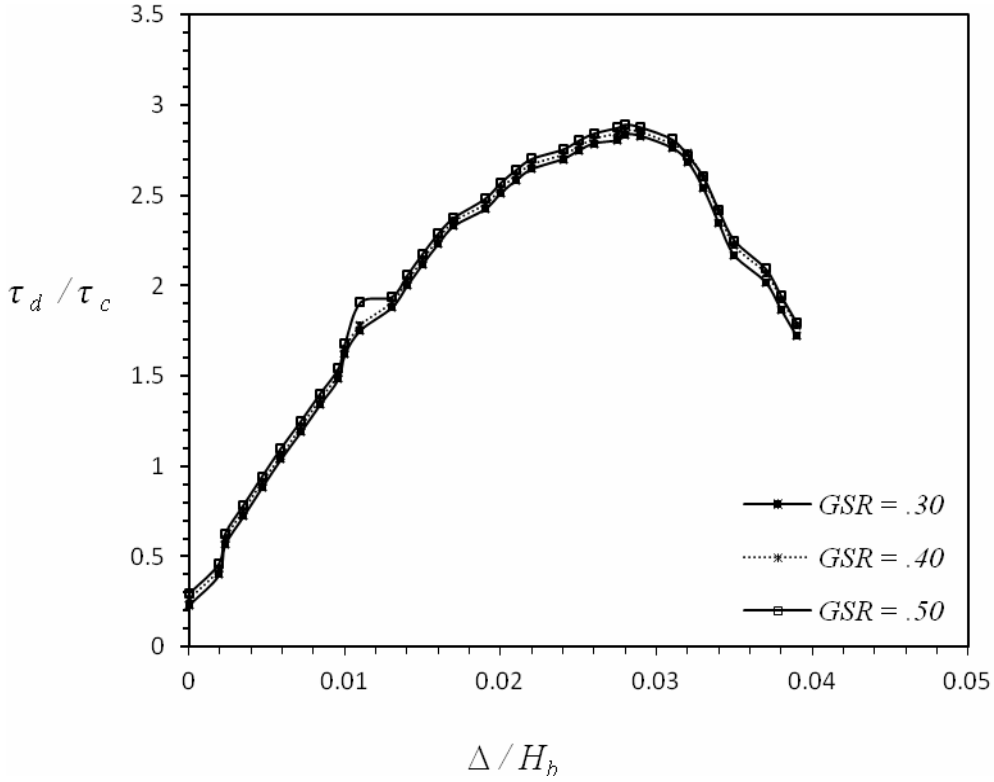

Figure 5.4. Variation of shear demand with gravity shear ratio

-ate failure) showed a decreasing trend up to critical depth to span ratio (*i.e.*, $d/L = 0.08$, $c_{dr} = 1$). For $c_{dr} > 1$, the trend reverses as Δ_{max} increases with increase in the value of d/L. The shear capacity of the connection increased with increase in lateral confinement pressure around the concrete (*i.e.*, with decrease in spacing of stirrups). The lateral drift capacity, Δ_{max} was found to be independent of the confinement pressure and was observed to be around 6%. Both the ductility and strength of the connection got enhanced with increase in confinement pressure. The IS code prescribed elastic drift limit of 0.4% underestimates the actual behaviour. The elastic drift limit ($\Delta_{elastic}$) is found to be independent of aspect ratio, span to depth ratio and confining pressure. The shear stress demand of the connection increases with increase in gravity shear ratio.

7. ACKNOWLEDGEMENTS

The work reported here has been carried out as part of the Master of Technology research. The authors would like to thank the Civil Engineering Department of IIT Guwahati for making available all the computing facilities and reference papers.

REFERENCES

CSI (2009), SAP2000 Version 14.2. Linear and Nonlinear Static and Dynamic Analysis and Design of Three-Dimensional Structures, Computers and Structures Inc., Berkeley, USA.

Dasgupta, P. (2000). Effect of Confinement on Strength and Ductility of Large RC Hollow Sections. Master of Technology Thesis, Indian Institute of Technology Kanpur, India.

IS:1893 (Part 1)-2002 (2002). Indian Standard Criteria for Earthquake Resistant Design of Structures - Part 1: General Provisions and Buildings, Bureau of Indian Standards, India.

IS 456:2000 (2005), Plain and Reinforced Concrete - Code of Practice, Bureau of Indian Standards, New Delhi.

Kashliwal, A. (2011). Seismic Behaviour of Reinforced Concrete Flat Plate Systems. Master of Technology Project, Department of Civil Engineering, Indian Institute of Technology Guwahati, India.

Kuang, J.S. and Morley, C T. (1992). Punching shear behavior of restrained reinforced concrete slabs. *ACI Structural Journal* **89:1**, 13-19.

Park, H. and Choi, K. (2006). Improved Strength Model for Interior Flat-Plate Column Connections Subject to Unbalanced Moment. *ACI Structural Journal* **23:3,** 694-704.

Saatcioglu, M. and Razvi, S.R. (1992). Strength and Ductility of Confined Concrete. *Journal of Structural Engineering ASCE* **118:1**, 1590-1607.

Yankelevsky, D. and Leibowitz, O. (1995). Punching shear in concrete slabs. *International Journal of Mechanical Sciences* **41:1**, 1-15.

Zhang, X. (2002). Punching Shear Failure Analysis of Reinforced Concrete Flat Plates using simplified UST failure criteria. Master of Technology Thesis, School of Engineering Faculty and Information Technology, Griffith University Gold Coast Campus.